

RIR-MAPLE deposition of plasmonic silver nanoparticles

Wangyao Ge¹ · Thang B. Hoang^{2,3} · Maiken H. Mikkelsen^{1,2,3} ·
Adrienne D. Stiff-Roberts¹

Received: 28 May 2016 / Accepted: 8 August 2016
© Springer-Verlag Berlin Heidelberg 2016

Abstract Nanoparticles are being explored in many different applications due to the unique properties offered by quantum effects. To broaden the scope of these applications, the deposition of nanoparticles onto substrates in a simple and controlled way is highly desired. In this study, we use resonant infrared matrix-assisted pulsed laser evaporation (RIR-MAPLE) for the deposition of metallic, silver nanoparticles for plasmonic applications. We find that RIR-MAPLE, a simple and versatile approach, is able to deposit silver nanoparticles as large as 80 nm onto different substrates with good adhesion, regardless of substrate properties. In addition, the nanoparticle surface coverage of the substrates, which result from the random distribution of nanoparticles across the substrate per laser pulse, can be simply and precisely controlled by RIR-MAPLE. Polymer films of poly(3-hexylthiophene-2,5-diyl) (P3HT) are also deposited by RIR-MAPLE on top of the deposited silver nanoparticles in order to demonstrate enhanced absorption due to the localized surface plasmon resonance effect. The reported features of RIR-MAPLE nanoparticle deposition indicate that this tool can enable efficient processing of nanoparticle thin films for applications that require specific substrates or configurations that are not easily achieved using solution-based approaches.

1 Introduction

The simple, benchtop synthesis of nanoparticles has facilitated studies of these materials applied to a variety of fields [1, 2]. Over the past 20 years, nanoparticles have been used for solar cells [3], LEDs [4], photodetectors [5], drug delivery [6] and plasmonics [7, 8]. With respect to the synthesis of colloidal nanoparticles, one important step is to incorporate organic ligands that prevent nanoparticles from aggregating during growth [9]. In addition, these organic ligands passivate the nanoparticle surface and can determine the solubility of the nanoparticles. Due to a broad range of compatible solvents, nanoparticles can be deposited as pure or blended films by straightforward, laboratory techniques for thin-film deposition, such as drop-casting or spin-casting. For drop-casting, the deposited nanoparticle films are not uniform, with large variance in the thickness across the films. The spin-cast method usually yields more uniform nanoparticle films; however, it is challenging to deposit thick films with a single-layer spin procedure due to the low viscosity of the nanoparticle solution that results in poor attachment to the substrate surface. Thus, despite the many benefits of these simple thin-film deposition techniques, the resulting nanoparticle films are far from ideal.

More recent solution-based processing techniques for nanoparticle thin films include the multi-layer spin-casting procedure for thick nanoparticle films, in which surface ligands are removed from a deposited film to prevent the dissolution of the previous layer during spin-casting of the next layer [10]. Other methods, such as self-assembly [11] and adsorption of nanoparticles onto oppositely charged substrates [12], provide precise control of the nanoparticle film. Yet, these techniques are specifically designed for certain substrates or nanoparticle material systems. One

✉ Adrienne D. Stiff-Roberts
adrienne.stiffroberts@duke.edu

¹ Department of Electrical and Computer Engineering, Duke University, Durham, NC 27708, USA

² Department of Physics, Duke University, Durham, NC 27708, USA

³ Center for Metamaterials and Integrated Plasmonics, Duke University, Durham, NC 27708, USA

way to circumvent the challenges of solution-based processing is to deposit nanoparticles in a “dry” state. Vacuum-based deposition of nanoparticle films could avoid problems arising from the wetting/dewetting of nanoparticles on the substrate and the possible redissolution issues encountered by the multi-layer spin-casting method.

In previous studies, the pulsed laser deposition (PLD) technique has been applied to deposit silver nanoparticles from a solid silver target, in which the generation of nanoparticles occurs during the course of the laser–target interaction [13–15]. In this paper, we employed resonant infrared matrix-assisted pulsed laser evaporation (RIR-MAPLE), another vacuum-based approach, to deposit as-synthesized silver nanoparticles. In contrast to PLD, RIR-MAPLE does not generate silver nanoparticles during the deposition. Instead, it transfers the as-synthesized silver nanoparticles from the target onto the substrate. This ability to directly transfer as-synthesized nanoparticles has two important features. First, we can still take advantage of the versatility of colloidal chemistry to deposit a wide range of nanoparticles, such as core–shell nanoparticles or nanoparticles with unique organic ligands for functionalization. In contrast, the types of nanoparticles that can be deposited by PLD are limited by the solid target. Second, we can blend nanoparticles with polymers using sequential deposition by RIR-MAPLE [16]; however, this is difficult to achieve by PLD because the process degrades the polymer during deposition. While RIR-MAPLE is a variation of pulsed laser deposition (PLD), it has two distinguishing aspects. First, the target for laser irradiance is not a pure solid material; instead, the guest material (e.g., silver nanoparticles) is dissolved into a matrix solvent (e.g., de-ionized (DI) water) that is subsequently frozen to form a solid target. Second, the laser is not a high energy, ultrafast UV-laser, but a lower energy infrared laser (Er:YAG) with a pulse width of 90 μ s and a peak wavelength of 2.94 μ m that is resonant with a specific vibrational mode frequency in the matrix solvent ($-\text{OH}$ bond). Therefore, the laser energy is absorbed primarily by the matrix solvent, which minimizes degradation of the guest material (both photochemical and structural).

Previous studies have shown the ability of MAPLE-based techniques to deposit TiO_2 [17], SnO_2 [18] and CdSe [19] nanoparticles for different applications such as gas sensors [20] and solar cells [16]. In this paper, we use RIR-MAPLE to deposit silver nanoparticles for plasmonic applications. We show that by using RIR-MAPLE for thin-film deposition, relatively large silver nanoparticles (~ 80 nm) could be deposited onto different types of substrates. In addition, the surface coverage of the silver nanoparticles can be precisely controlled by tuning the target concentration and/or deposition time in the RIR-MAPLE process. Finally, RIR-MAPLE was used to deposit

a bi-layer film of silver nanoparticles coated with a conjugated polymer film of poly(3-hexylthiophene-2,5-diyl) (P3HT), which showed enhanced absorption compared to the P3HT film alone. The results of these studies indicate the power of the RIR-MAPLE technique to deposit nanoparticles in a general and controlled manner that can be applied to a broad range of nanoparticle/substrate material systems, as well as integrated with polymeric thin films in multi-layer structures.

2 Experimental details

The synthesis of silver nanoparticles followed previous reported procedures [21, 22] with slight modification [23]. In short, a round-bottom flask with a 5 mL of ethylene glycol and mixture of the following four chemicals (also dissolved in ethylene glycol): sodium hydrosulfide hydrate (NaSH 1.3 mM, 60 μ L), poly vinylpyrrolidone (PVP 20 mg/mL, 1.25 mL), hydrochloric acid (HCL 2.5 μ M, 500 μ L) and silver trifluoroacetate ($\text{AgC}_2\text{F}_3\text{O}_2$ 0.0623 g/mL, 400 μ L) was heated and stirred (260 rpm) in a hot oil bath at 150 $^\circ\text{C}$. The heating time determines the size of the nanocubes. This synthesis enables the fabrication of nanocubes with side lengths ranging from 50 to 100 nm. For example, in this present work, a heating time of 2.5 h was used and resulted nanocubes have side lengths of ~ 75 nm with slightly rounded corners (radius of curvature ~ 10 nm). A longer synthesis time (>3 h) will lead to larger nanoparticles; however, this may also result in different shapes such as truncated nanocubes or octahedrons. The final solution was centrifuged and re-suspended in deionized water and may be stored for at least 1 month in a fridge at 4 $^\circ\text{C}$ without any noticeable changes in the plasmon resonances [24].

The deposition of silver nanoparticles was based on standard techniques [25, 26]. First, the as-synthesized silver nanoparticle solution was diluted by DI water to achieve the desired concentration. It is important to note that the maximum silver nanoparticle concentration used was 3 mg/mL, which corresponds to a total volume of 0.0023 cm^3 , assuming the bulk density of silver nanoparticles is 1.3 g/cm^3 . This volume is three orders of magnitude less than that for the water matrix, which surrounds the nanoparticles as a continuous phase. Next, the prepared solution (6 mL total) was injected into the chilled target cup (-190 $^\circ\text{C}$, cooled by liquid nitrogen) using a syringe. After target preparation, the chamber was evacuated and the laser was turned on to irradiate the frozen target for different deposition times. The incident laser fluence was 1.8 J/cm^2 per pulse with a 2 Hz repetition rate. Considering the absorption coefficient of water ice at the laser fluence used during deposition (~ 2000 cm^{-1}) [27, 28], the laser

irradiance drops to $1/e$ of the original value after 5 μm distance, so most of the laser energy is absorbed by water before reaching the silver nanoparticles. The substrate temperature was not actively controlled (which means it was below freezing due to the target cold block in vacuum), and the target-to-substrate distance was maintained at 7 cm.

The deposition of P3HT films by RIR-MAPLE followed a similar procedure to that for the silver nanoparticles, with the exception that an emulsion target was used. The emulsion contained: (1) 1,2,4-trichlorobenzene (TCB) as the primary solvent to dissolve P3HT, (2) phenol as the secondary solvent to both enrich the $-\text{OH}$ bond in the emulsion and stabilize the emulsion under the high vacuum, and (3) DI water with 0.001 wt% sodium dodecyl sulfate (SDS) to complete and stabilize the emulsion, as well as provide the main contribution of $-\text{OH}$ bonds to absorb the incident laser energy. The volume ratio between TCB, phenol, and water was 1:0.25:3.

The SEM images were obtained using an FEI XL30 SEM with 30 kV voltage. The surface coverage of silver nanoparticles was defined as the ratio of the area of silver nanoparticles to the total area of the SEM image and was calculated by ImageJ. The UV-Vis extinction/absorbance spectra were obtained using a Shimadzu UV-3600 spectrophotometer.

3 Results and discussion

One disadvantage of solution-processed deposition techniques is that the formation of the films heavily depends on substrate wetting/dewetting processes. Good wettability of the solution on the underlying substrate is essential to form a uniform film. This is especially important for nanoparticle film deposition, in which the low viscosity of the solution already limits nanoparticle attachment to the substrate. Therefore, the surface tension of the solution must be carefully designed in order to deposit the nanoparticle film onto a specific type of substrate. On the other hand, the RIR-MAPLE technique offers a very simple and general method to deposit nanoparticles onto different types of substrates using the same deposition parameters. Figure 1a shows photographs of silver nanoparticle films deposited by RIR-MAPLE onto a variety of substrates, including inorganic substrates (silicon, glass), metallic substrates (aluminum foil), plastic substrates (scotch tape, parafilm), and a paper substrate. The origin of the general applicability of the RIR-MAPLE deposition process, regardless of underlying substrates, is that it is a “dry” deposition technique compared to solution-processed deposition techniques. Ideally, in the silver nanoparticle deposition, the frozen matrix solution is pure

water, which absorbs the laser energy, is vaporized, and pumped away in the evacuated chamber, leaving the nanoparticles to transfer to the substrate in a “dry” state. In reality, a minimal amount of water molecules could be co-deposited onto the substrate [29], but the amount of water molecules does not result in any wettability issues similar to solution-processed deposition techniques, as evidenced by the deposited films. This “dry” deposition method enables the deposition of nanoparticles onto different substrates and eliminates the need to consider the compatibility between the nanoparticle solvent and substrate. As a specific example, paper substrates, which are good absorbers for most solvents, are not appropriate for solution-processing; yet, RIR-MAPLE can deposit a high-quality silver nanoparticle film without detrimental impact on the paper substrate. Figure 1b summarizes the RIR-MAPLE process, in which laser irradiation of a frozen silver nanoparticle/water solution results in the “dry” deposition of a silver nanoparticle film. It can be seen from the top SEM image in Fig. 1b that the silver nanoparticles are deposited onto the substrate randomly, stacked one-by-one or cluster-by-cluster, without any identifiable pattern. Figure 1c shows the normalized extinction spectra of as-synthesized silver nanoparticles in solution and a silver nanoparticle film deposited onto glass by RIR-MAPLE. From the extinction spectra, it can be seen that, whereas the peak position is identical, the width of the extinction peak of the silver nanoparticle film is much narrower than that of the silver nanoparticle solution, indicating that the silver nanoparticle size distribution in the deposited film is more monodisperse than the silver nanoparticles in the solution. Given that it is possible for silver nanoparticles to resonantly absorb some of the laser energy, a small portion of silver nanoparticles may have been etched away from the target, resulting in a more uniform size distribution; however, as indicated by the extinction coefficient peak after film deposition, most of the nanoparticles are deposited intact. From the film extinction spectrum, the primary peak is around 460 nm in the visible range. The secondary peak near 400 nm arises from a quadrupole resonance, a different electron oscillation frequency compared to the primary dipole resonance [30]. These optical properties of silver nanoparticle films indicate that RIR-MAPLE deposited silver nanoparticles are suitable to enhance the absorption of a polymer with a HOMO-LUMO gap in the visible range, such as P3HT.

RIR-MAPLE also offers a simple way to control the surface coverage of silver nanoparticles on a substrate by tuning either the silver nanoparticle concentration in the frozen target or the deposition time. Figure 2a shows the relation between surface coverage of silver nanoparticles on silicon substrates and the silver nanoparticle target concentration or deposition time. Specifically, the silver

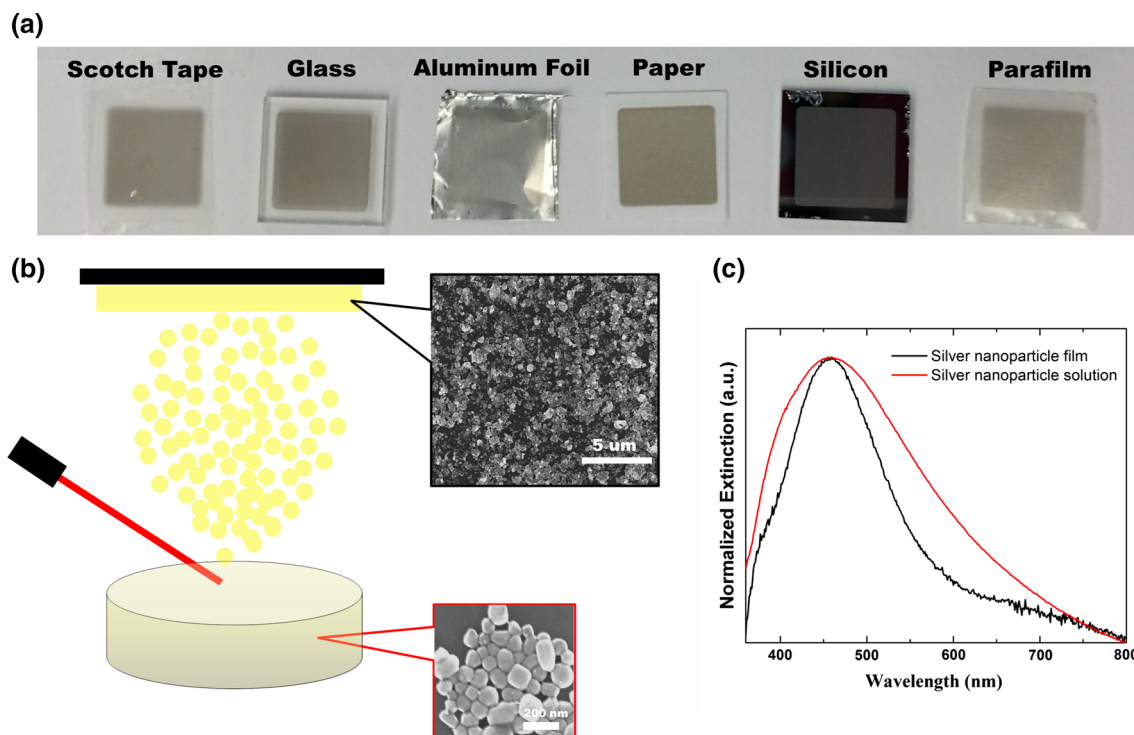


Fig. 1 **a** Silver nanoparticle films deposited by RIR-MAPLE onto different types of substrates. **b** Schematic representation of RIR-MAPLE process, in which silver nanoparticles in the target are deposited onto the substrate. The *bottom* SEM image shows the as-

synthesized silver nanoparticles, and the *top* SEM image shows the deposited silver nanoparticles on the silicon substrate. **c** The extinction (absorption + scattering) spectrum of silver nanoparticles in solution and deposited as a solid film on the glass substrate

nanoparticles are deposited from the RIR-MAPLE targets with concentrations of 0.75, 1.5 or 3 mg/mL. For each concentration, three films are deposited for times of 1, 2 and 3 h. The surface coverage, which is defined as the percentage of silver nanoparticle area to the total area of the image, is determined from SEM images using ImageJ. From the figure, it can be seen that the surface coverage is linearly proportional to both target concentration and deposition time. Therefore, any surface coverage can be obtained by carefully selecting the calibrated target concentration and deposition time. Figure 2b shows the extinction spectra of silver nanoparticle films with different surface coverage, demonstrating that the resonant peak intensity varies linearly with the silver nanoparticle surface coverage, while the peak wavelength does not. Usually, the aggregation of silver nanoparticles induces a red shift in the resonant peak wavelength and decreases the resonant peak intensity. Therefore, the increasing peak intensity and unchanged peak position indicate that the RIR-MAPLE technique does not increase the silver nanoparticle aggregation, even as the surface coverage is increased. Figure 2c shows SEM images of silver nanoparticle films with three different surface coverage values. From the SEM images, aggregated silver nanoparticle clusters are observed, which occur due to the transfer of silver nanoparticle aggregates from the water solution due to the RIR-MAPLE deposition process.

In recent studies, the localized surface plasmon resonance (LSPR) effect of metal nanoparticles has been explored to enhance the absorption of thin films, and it has been applied to increase the efficiency of solar cells [31, 32]. The LSPR effect of metal nanoparticles occurs when the frequency of incoming light matches the frequency of oscillating free electrons in the nanoparticles, resulting in both enhanced scattering and enhanced absorption of the light. For silver nanoparticles, the optimal nanoparticle size is around 80 nm, which results in dominant forward light scattering that enhances absorption in the solar cell active region by increasing the optical path length [31]. For plasmonic organic solar cells, depending on the solubility characteristics of silver nanoparticles, they are either co-dissolved into the hydrophilic hole transport layer solution of poly(3,4-ethylenedioxythiophene)-poly(styrenesulfonate) (PEDOT:PSS) or the hydrophobic organic active region solution, from which thin films of the nanocomposite are formed by spin-casting [32]. For RIR-MAPLE deposition, the solubility characteristic of the silver nanoparticles does not impact the location at which they can be incorporated because RIR-MAPLE is a “dry” deposition process. To test the plasmonic effect of silver nanoparticle films deposited by RIR-MAPLE, the absorbance spectra of RIR-MAPLE deposited P3HT films on bare glass substrates, with and without silver nanoparticles,

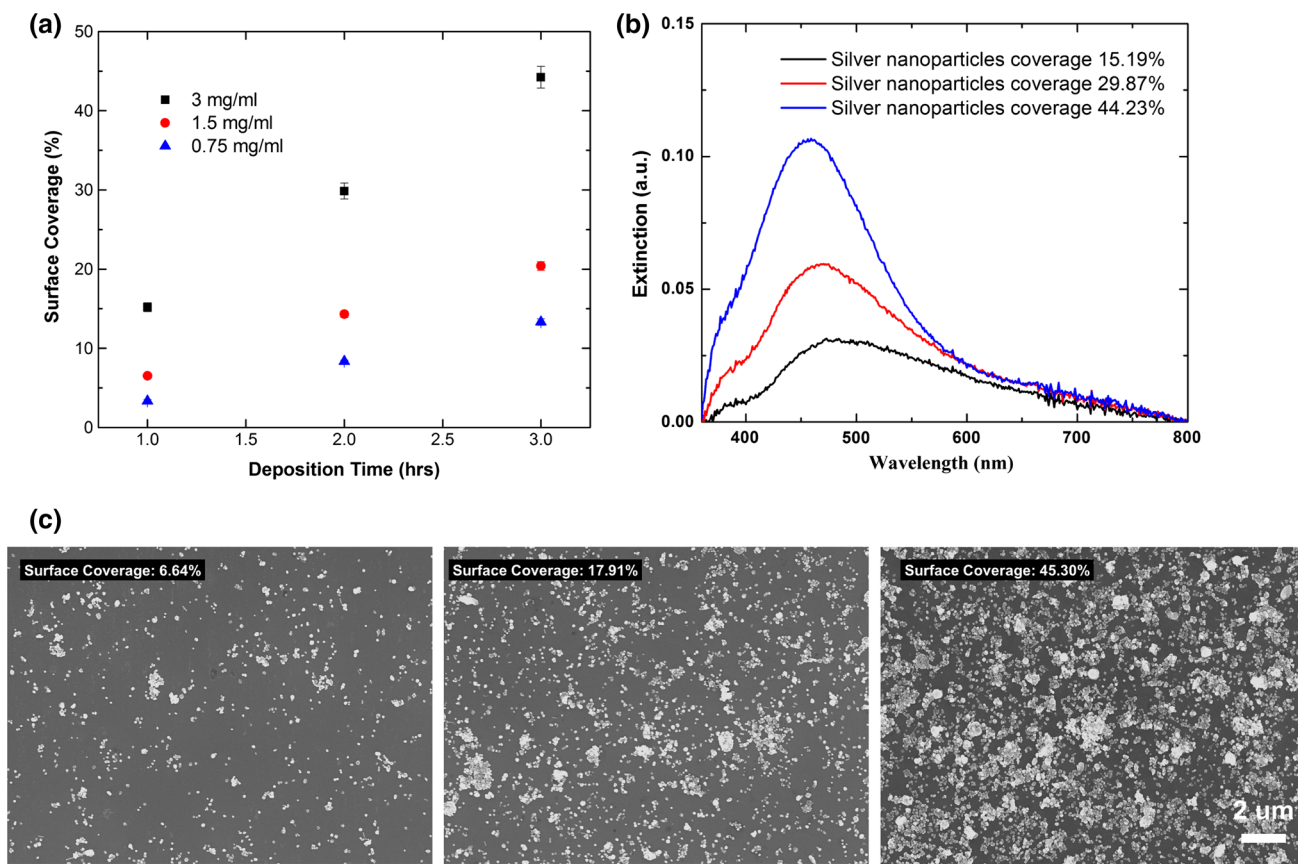


Fig. 2 **a** Silver nanoparticles deposited by RIR-MAPLE using different target concentration and deposition time. Each surface coverage point is obtained by averaging six SEM images, and the error bar represents the standard deviation of surface coverage. **b** The

extinction spectra of silver nanoparticle films with different surface coverage. **c** SEM images of silver nanoparticle films with three different surface coverage values

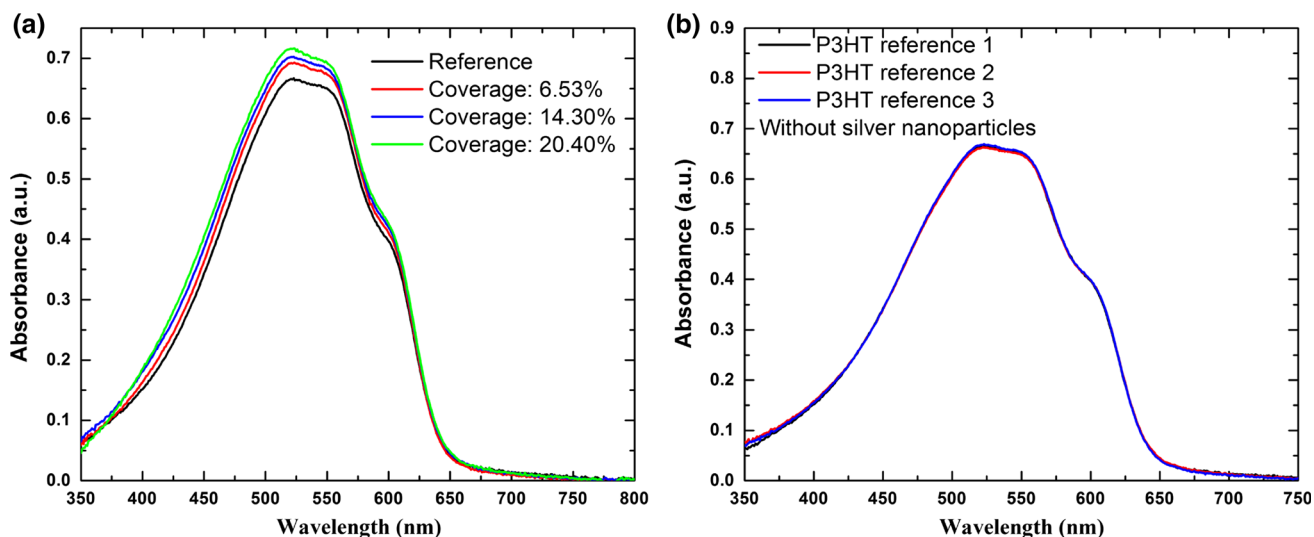


Fig. 3 **a** The absorbance spectra of P3HT films deposited onto glass substrates with and without different silver nanoparticle surface coverage. **b** The absorbance spectra of three reference P3HT films.

The identical absorbance intensity indicates the enhanced absorption is due to the plasmonic effect, not thickness variation in different P3HT films

are compared. Figure 3 a shows the absorbance spectra of P3HT films on a bare glass substrate and on the glass substrate with three different silver nanoparticle surface coverage. Clearly, enhanced absorption is observed when more silver nanoparticles are incorporated on the glass substrate, underneath the P3HT film, indicating that RIR-MAPLE does not compromise the plasmonic properties of silver nanoparticles. It is worth mentioning that the consistency of the RIR-MAPLE process helps avoid any misinterpretation of the results due to measurement error. For example, the substrate holder can accommodate six substrates for a single P3HT film deposition such that the deposition conditions for each of the six substrates are identical. Three of the six substrates were reference samples with bare glass substrates, and the remaining three samples had films of different silver nanoparticle surface coverage. From Fig. 3b, it can be seen that the reference P3HT samples show exactly the same absorption intensity, indicating the enhanced absorption of P3HT on the three substrates with silver nanoparticle films results from the plasmonic effect, not variation of the P3HT film thickness.

4 Summary

In summary, RIR-MAPLE is demonstrated to be a simple and general technique to deposit silver nanoparticles for plasmonic applications. The precise control of the amount of nanoparticles deposited onto any type of substrates, without compromising nanoparticle properties, is the key feature of the RIR-MAPLE technique. This versatile approach is attractive for the deposition of nanoparticles for special applications that require specific substrates or configurations.

Acknowledgments This work was supported by the Duke University Energy Initiative Energy Research Seed Fund and the Duke University Pratt School of Engineering.

References

1. H. You, S. Yang, B. Ding, H. Yang, *Chem. Soc. Rev.* **42**, 2880 (2013)
2. Y. Yin, A.P. Alivisatos, *Nature* **437**, 664 (2005)
3. G.H. Carey, A.L. Abdelhady, Z. Ning, S.M. Thon, O.M. Bakr, E.H. Sargent, *Chem. Rev.* **115**, 12732 (2015)
4. Y. Shirasaki, G.J. Supran, M.G. Bawendi, V. Bulovic, *Nat. Photonics* **7**, 13 (2013)
5. P. Martyniuk, A. Rogalski, *Prog. Quantum Electron.* **32**, 89 (2008)
6. P. Couvreur, *Adv. Drug Deliv. Rev.* **65**, 21 (2013)
7. A. Sanchot, G. Baffou, R. Marty, A. Arbouet, R. Quidant, C. Girard, E. Dujardin, *ACS Nano* **6**, 3434 (2012)
8. W. Hou, S.B. Cronin, *Adv. Funct. Mater.* **23**, 1612 (2013)
9. C.M. Evans, L.C. Cass, K.E. Knowles, D.B. Tice, R.P.H. Chang, E.A. Weiss, *J. Coord. Chem.* **65**, 2391 (2012)
10. C.H. Chuang, P.R. Brown, V. Bulovic, M.G. Bawendi, *Nat. Mater.* **13**, 796 (2014)
11. M. Brust, D.J. Schiffrin, D. Bethell, C.J. Kiely, *Adv. Mater.* **7**, 795 (1995)
12. M.D. Musick, C.D. Keating, L.A. Lyon, S.L. Botsko, D.J. Peña, W.D. Holliday, T.M. McEvoy, J.N. Richardson, *Chem. Mater.* **12**, 2869 (2000)
13. U. Gurudas, E. Brooks, D.M. Bubb, S. Heiroth, T. Lippert, A. Wokaun, *J. Appl. Phys.* **104**, 073107 (2008)
14. T. Yamamoto, K. Machi, S. Nagare, K. Hamada, M. Senna, *Solid State Ion.* **172**, 299 (2004)
15. J.C. Alonso, R. Diamant, P. Castillo, M.C. Acosta-García, N. Batina, E. Haro-Poniatowski, *Appl. Surf. Sci.* **255**, 4933 (2009)
16. W. Ge, A. Atewologun, A.D. Stiff-Roberts, *Org. Electron.* **22**, 98 (2015)
17. A.P. Caricato, M.G. Manera, M. Martino, R. Rella, F. Romano, J. Spadavecchia, T. Tunno, D. Valerini, *Appl. Surf. Sci.* **253**, 6471 (2007)
18. A.P. Caricato, M. Epifani, M. Martino, F. Romano, R. Rella, A. Taurino, T. Tunno, D. Valerini, *J. Phys. D Appl. Phys.* **42**, 095105 (2009)
19. R. Pate, K.R. Lantz, A.D. Stiff-Roberts, *Thin Solid Films* **517**, 6798 (2009)
20. A.P. Caricato, A. Luches, R. Rella, *Sensors* **9**, 2682 (2009)
21. S.E. Skrabalak, L. Au, X. Li, Y. Xia, *Nat. Protoc.* **2**, 2182 (2007)
22. Q. Zhang, W. Li, L.P. Wen, J. Chen, Y. Xia, *Chem. Eur. J.* **16**, 10234 (2010)
23. T.B. Hoang, J. Huang, M.H. Mikkelsen, *J. Vis. Exp.* **111**, e53876 (2016)
24. A. Rose, T.B. Hoang, F. McGuire, J.J. Mock, C. Ciraci, D.R. Smith, M.H. Mikkelsen, *Nano Lett.* **14**, 4797 (2014)
25. R. Pate, K.R. Lantz, A.D. Stiff-Roberts, *IEEE J. Sel. Top. Quantum Electron.* **14**, 1022 (2008)
26. W. Ge, R.D. McCormick, G. Nyikayaramba, A.D. Stiff-Roberts, *Appl. Phys. Lett.* **104**, 223901 (2014)
27. R. Pate, A.D. Stiff-Roberts, *Chem. Phys. Lett.* **477**, 406 (2009)
28. G.M. Hale, M.R. Querry, *Appl. Opt.* **12**, 555 (1973)
29. E. Leveugle, L.V. Zhigilei, *J. Appl. Phys.* **102**, 074914 (2007)
30. D.D. Evanoff Jr., G. Chumanov, *ChemPhysChem* **6**, 1221 (2005)
31. S.W. Baek, J. Noh, C.H. Lee, B. Kim, M.K. Seo, J.Y. Lee, *Sci. Rep.* **3**, 1726 (2013)
32. F.X. Xie, W.C.H. Choy, C.C.D. Wang, W.E.I. Sha, D.D.S. Fung, *Appl. Phys. Lett.* **99**, 153304 (2011)